Project Thesis

Solving the Biharmonic Equation using

a Continuous Interior Penalty Method

Isak Hammer

Supervisor: André Massing

Department of Mathematical Sciences

Norwegian University of Science and Technology

July 1, 2022

1 Introduction

The biharmonic equation is a fourth order partial differential equation which has gained great importance in application such as mathematical modelling of linear elastic theory [1] and phase separation mechanics of two phase systems [2, 3]. However, methods for solving the biharmonic equation analytically is considered extensive and often impossible. Even for very simple plane problems on a unit square often requires advanced computations using integral transforms, variable separations, complex analysis and more [1]. We therefore tend to lean towards approximating the solution using numerical methods for complicated problems.

There is generally two classes of numerical methods to solve the biharmonic equation. The first class is known as finite difference method (FDM) [4–6]. Nevertheless, FDM does not handle complex domains well since it generally has strict requirements for the mesh generation. However, some methods have been introduced to solve problems on irregular domains, but is has shown to be relative extensive to implement [6–8].

The second class is denotes as finite element method (FEM). Using this methods implies that there is theoretically no difference between solving problems on a regular or on an irregular domain, except for taking account for numerical stability and some restrictions on mesh generation [7]. However, a major challenge in FEM is to choose a discrete solution space on the finite elements to approximate the exact solution. We say that a method is conforming if the discrete solution space V_h is subspace of the exact solution space V, i.e. $V_h \subseteq V$ [9, 10]. In general, for conforming methods requires that for a problem of order $2n$ must the discrete solution space be at least C^{n-1}, i.e., $(n-1)$ times continuously differentiable. Thus, for a biharmonic problem will a conforming FEM method demand at least a basis that is C^1 globally [9]. From this strong continuity conditions rises a lot of complexity when constructing a finite element. In fact, attempts to solve this problems has shown that it arise 21 degrees of freedom in a triangular Argyris element [11].

For nonconforming methods, $V_h \not\subseteq V$, the C^1 requirement is completely relaxed. This makes the methods more suitable for fourth order problems at the cost of a more extensive error analysis. In fact, designing nonconformal elements that does converge is rather difficult [9, 11].

A third approach of FEM to solve the biharmonic equation is to solve the problem applying a mixed FEM method. This method seems promising, because it only requires C^0 elements [7, 12]. Though this works well from a numerical point of view, it has shown to have drawbacks by replacing symmetric positive definite continuous problem by a saddle point problem, which is certainly makes the existence and uniqueness proof more challenging, as well as the design of efficient preconditioner [13].

In this report will we focus to work on a fourth approach known as the continuous interior penalty method (CIP). A major advantage is that the approach preserves the global C^0 continuity and the positive symmetric definiteness, thus makes it attractive to solve the biharmonic equation [14, 15]. The goal of this report is to give a detailed account on the derivations of CIP and its a priori error analysis following the presentations in [14, 16]. We will also present a basic numerical analysis.

2 Mathematical Background

In this section will we briefly establish some basic results of functional analysis and numerical analysis in order to construct the foundations of the FEM method. However, for a more thoroughly explanation some recommended sources are [10, 17, 18]. We will first define basic principles of Hilbert spaces which then will be applied to establish a theory for weak formulations and the notion of a well posed problem. Moreover, we will then continue by establishing error estimates and constructing a numerical discretization of the weak formulation using a simple test problem.

2.1 Hilbert Spaces

We will generally in section 2 assume Ω to be a compact and open set in $\mathbb{R}^2$. Now let the parameter $p \in \mathbb{R}$, $p \geq 1$. We then define the space $L^p(\Omega)$ to be the set of all measurable functions $f : \Omega \mapsto \mathbb{R}$ such that $|f|^p$ is Lebesgue measurable, i.e,

$$L^p(\Omega) = \left\{ f : \Omega \mapsto \mathbb{R} \mid \int_\Omega |f|^p \, d\Omega < \infty \right\}.$$

A useful extension, which we will use later, are the set of locally integrable functions for any compact subset $K \subseteq \text{Interior}(\Omega)$ [10], that is,

$$L^1_{loc}(\Omega) = \left\{ f : f \in L^1(\Omega) \quad \forall K \right\}.$$

Let $u \in L^p(\Omega)$. We define the integral norm of order p to be

$$\|u\|_{L^p(\Omega)} = \left(\int_\Omega |u|^p \, dx \right)^{\frac{1}{p}}.$$

Since $p = 2$ is frequently used in this report, we also define for convenience a compact notation $\|u\|_\Omega = \|u\|_{L^2(\Omega)}$. We say that $L^2(\Omega)$ is a Hilbert space if it is equipped with a inner product of two functions $u, v \in L^2(\Omega)$ such that

$$(u, v)_\Omega = (u, v)_{L^2(\Omega)} = \int_\Omega uv dx.$$

To generalize, we denote the notation $\mathcal{V}$ for a arbitrary Hilbert space. Furthermore, we define the dual space the be the space of linear and bounded functionals $F : \mathcal{V} \mapsto \mathbb{R}$[18], i.e.,

$$\mathcal{V}^* = \left\{ \begin{array}{l} F : \mathcal{V} \mapsto \mathbb{R} \text{ such that } \forall v, w \in \mathcal{V}, \forall a, b \in \mathbb{R} \text{ and } C > 0 \text{ is} \\ F(\lambda v + \mu w) = \lambda F(v) + \mu F(w) \text{ and } |F(v)| \leq C \|v\|_{\mathcal{V}} \end{array} \right\}$$

and we equip it with the functional norm,

$$\|F\|_{\mathcal{V}^*} = \sup_{v \in \mathcal{V}} \frac{|F(v)|}{\|v\|_{\mathcal{V}}}.$$

We will now establish a notion of the weak derivative, but first are we going to characterize some useful definitions of continuity. The space $C^k(\Omega)$ for $k \geq 0$ denotes the set of functions whose derivatives, up to order of k , is continuous in Ω. Note that we often use the shorthand notation $C^0 = C(\Omega) = C^0(\Omega)$. From this, let $C^\infty(\Omega)$ be the set of infinitely differentiable functions in Ω. Furthermore, we then denote the space $C_0^\infty(\Omega)$ as the space of all functions, $u \in C^\infty(\Omega)$, vanishing outside of any compact subset of Ω. Let $u, v \in C^1(\Omega)$ and the define boundary $\Gamma = \partial\Omega$ with a corresponding outer normal vector n. It is well known that this partial integration formula holds [17],

$$\int_\Omega \nabla u \cdot v dx = \int_\Gamma u \cdot v n ds - \int_\Omega u \cdot \nabla v dx.$$

We now use this notation for derivatives [1] so

$$\partial^\alpha f = \frac{\partial^{|\alpha|} f}{\partial^{\alpha_1} x_1 \partial^{\alpha_2} x_2}, \quad \text{where } \alpha = (\alpha_1, \alpha_2) \text{ and } f \in C^{|\alpha|}(\Omega). \tag{1}$$

[1] In literature is often $D^\alpha f$ commonly used, but later in the report is this notation reserved for the Hessian operator. Therefore, we then the notation $\partial^\alpha f$ in this report.

Finally, let $u \in L^1_{loc}(\Omega)$. We call the function $w \in L^1_{loc}(\Omega)$ the α-th weak derivative of u if

$$\int_\Omega w\varphi dx = (-1)^{|\alpha|} \int_\Omega u \cdot \partial^\alpha \varphi dx, \quad \forall \varphi \in C_0^\infty(\Omega).$$

We are now able to construct the Sobolev space [17],

$$H^m(\Omega) = \left\{ u \in L^2(\Omega) \mid \partial^\alpha u \in L^2(\Omega) \, \forall \alpha : |\alpha| \leq m \right\} \text{ for } m > 1$$

Equipped with the inner product is $H^m(\Omega)$ denoted as a Hilbert space, that is, for $u, v \in H^m(\Omega)$,

$$(u, v)_{H^m(\Omega)} = \sum_{|\alpha| \leq m} \int_\Omega \partial^\alpha u \partial^\alpha v dx.$$

Similarly, the integral norm is denoted as,

$$\|u\|_{H^m(\Omega)} = \left(\|u\|_{L^2(\Omega)} + \sum_{k=1}^{m} |u|^2_{H^k(\Omega)} \right)^{\frac{1}{2}},$$

where the seminorm is defined such that,

$$|u|_{H^k(\Omega)} = \left(\sum_{|\alpha|=k} \|\partial^\alpha u\|^2_\Omega \right).$$

For convenience, we also entitle the notation,

$$H^m_0(\Omega) = \left\{ \text{completion of } C_0^\infty(\Omega) \text{ w.r.t. } \|\cdot\|_{H^m(\Omega)} \right\}.$$

2.2 Weak Formulation

By applying the theory of weak derivative it it possible describe the notion of a so-called weak formulation of a system. Let us consider a simple test problem, that is, the strong form of the Poisson's equation with homogeneous Dirichlet boundary conditions,

$$\begin{aligned} -\Delta u &= f \quad \text{in } \Omega \\ u &= 0 \quad \text{on } \partial\Omega \end{aligned}. \tag{2}$$

We want to obtain the weak formulation of the problem (2). Let the trial function be $u \in H^1_0(\Omega)$, then by integrating with a test function we get,

$$\int_\Omega -\Delta u \cdot v dx = \int_\Omega f \cdot v dx \quad \forall v \in H^1_0(\Omega).$$

By using the partial integration formula and take the advantage of homogeneous Dirichlet boundary conditions the equation can the formulation be simplified to

$$a(u,v) = \int_\Omega \nabla u \cdot \nabla v dx, \quad l(v) = \int_\Omega f v dx.$$

Thus, we say the final weak formulation is the problem where we want to find a solution $u \in H_0^1(\Omega)$ such that it fulfills the criteria

$$a(u,v) = l(v) \quad \forall v \in H_0^1(\Omega). \tag{3}$$

We now want to establish that problems on this form is well-posed. Lax-Milgram Theorem says that if we assume a Hilbert space $\mathcal{V}$ and a bilinear symmetric problem, where we want to find a $u \in \mathcal{V}$, such that

$$a(u,v) = (F,v)_{\mathcal{V}^*,\mathcal{V}}, \quad \forall v \in \mathcal{V} \text{ and } F \in \mathcal{V}^*.$$

Assume the bilinear form, $a(\cdot,\cdot)$, is continuous and coercive, i.e., the two conditions below.

1) There exists a constant $M > 0$ so that,

$$|a(v,w)| \leq M\|v\|_{\mathcal{V}}\|w\|_{\mathcal{V}} \quad \forall v,w \in \mathcal{V}.$$

2) There exists a $\alpha > 0$ so,

$$a(v,v) \geq \alpha \|v\|_{\mathcal{V}}^2.$$

If this is true, then there exists a unique solution, $u \in \mathcal{V}$, which satisfies the stability estimate [17],

$$\|w\|_{\mathcal{V}} \leq \|F\|_{\mathcal{V}^*}.$$

Problems that fulfills this criteria is said to be well posed.

Moreover, we can clearly see that this theorem is applicable to the weak formulation (3).

$$\begin{aligned} |a(v,w)| &\leq \|\nabla v\|_\Omega \|\nabla w\|_\Omega \leq \|v\|_{\mathcal{V}}\|w\|_{\mathcal{V}} \\ a(v,v) &= \frac{1}{2}\|\nabla v\|_\Omega^2 + \frac{1}{2}\|\nabla v\|_\Omega^2 \geq \beta\left(\|v\|_\Omega^2 + \|\nabla u\|_\Omega^2\right) \geq \beta\|v\|_{\mathcal{V}} \end{aligned}$$

Here is $\beta = \min\left\{\frac{1}{2}, \frac{1}{2C^2}\right\}$. In the last inequality was the Poincare inequality applied, i.e., there exists a $C > 0$ such that $\|v\|_\Omega \leq C\|\nabla v\|_\Omega$. Hence, the weak formulation (3) is well posed.

2.3 Ceas' Lemma

Since we have established a theory of a well-posed weak formulation we can now transition to setup a theory for a approximate solution. Assume that we have a problem that satisfies the Lax-Milgram theorem and let $\mathcal{V}_h \subseteq \mathcal{V}$ be some finite dimensional subspace of $\mathcal{V}$ such that $dim\,(\mathcal{V}_h) = N_h$, where h is a discretization parameter. We transition the problem to find a solution, $u_h \in \mathcal{V}_h$, such that,

$$a\,(u_h, v_h) = l\,(v_h) \quad \forall v_h \in \mathcal{V}_h.$$

Since the method is conform, i.e., $\mathcal{V}_h \subseteq \mathcal{V}$, does it exists a exact solution, $u \in \mathcal{V}_h$, so,

$$a\,(u, v_h) = l\,(v_h) \quad \forall v_h \in \mathcal{V}_h.$$

Furthermore, the problem is said to be strongly consistent since it fulfills the Galerkin orthogonality property, that is,

$$a\,(u - u_h, v_h) = 0.$$

Now we have all the cornerstones for computing a error estimate. Let $v_h \in \mathcal{V}_h$ so

$$\begin{aligned} \alpha\|u - u_h\|_{\mathcal{V}}^2 &\leq a\,(u - u_h, u - u_h) \\ &= a\,(u - u_h, u - v_h) - a\,(u - u_h, v_h - u_h). \\ &\leq M\|u - u_h\|_{\mathcal{V}}\|u - v_h\|_{\mathcal{V}} \end{aligned} \tag{4}$$

Hence, we now have the Ceas' lemma [18],

$$\|u - u_h\|_{\mathcal{V}} \leq \frac{M}{\alpha} \inf_{v_h \in \mathcal{V}} \|v_h - u\|.$$

A useful property is that for a conformal numerical method to converge can we now simply require

$$\lim_{h \to 0} \inf_{v_h \in V_h} \|v - v_h\|_{\mathcal{V}} = 0 \quad \forall v \in \mathcal{V}.$$

In that case will $\|u - u_h\|_{\mathcal{V}} \to 0$, $h \to 0$. Hence, if this requirement is fulfilled, the numerical methods will converge to a unique solution.

2.4 Finite Element Method

The idea of a conformal FEM method is to approximate a solution space, $\mathcal{V}_h \subseteq \mathcal{V}$. However, the building blocks of the discretization relies on constructing a triangulation

$\mathcal{T}_h$ with non-overlapping triangles, $T \in \mathcal{T}_h$, so that,

$$\Omega_h = Interior(\bigcup_{T \in \mathcal{T}_h} T) \implies \lim_{h \to 0} measure(\Omega - \Omega_h) = 0$$

For convenience, we will generally use the notation $\Omega = \Omega_h$ [2]. We also denote the parameter h as the diameter of the triangle T, i.e., $h_T = diam(T)$. Anyhow, this is later more precisely in the subsection 4.2, but as a basic introduction to FEM is this sufficient. Furthermore, let the space of finite elements suitable for our test problem in subsection 2.2 to be, by using the definition from [18],

$$\mathcal{V}_h = \left\{ v_h \in C^0(\Omega) \mid v_h \in \mathcal{P}_k(T) \quad \forall T \in \mathcal{T}_h \right\},$$

where $\mathcal{P}_k(T)$ is the space of polynomials with degree k for each T, that is,

$$\mathcal{P}_k(T) = \left\{ p(x_1, x_2) = \sum^{i+j} a_{ij} x_1^i x_2^j \mid a_{ij} \in \mathbb{R} \text{ and } i, j \geq 0 \right\}.$$

For the test problem can we observe that it is convenient to deal with a Lagrangian functions $\varphi_j \in V_h$. Thus, for every node N_j,

$$\varphi_j(N_i) = \delta_{ij} = \begin{cases} 0, & i \neq j \\ 1, & i = j \end{cases} \text{ where } i, j = 1, \ldots, N_h.$$

Here is N_h the total number of nodes which is chosen with caution. For the test problem, where $\Omega \subseteq \mathbb{R}^2$, then for $k = 1$ the nodes is typically defined on the vertices and for $k = 2$ is the nodes defined on the vertices and the center of the facets [18].

Finally, by using the set of basis functions, $\{\varphi_j\}$, can we discretize a solution, $u_j = u_h(N_j)$, so that $u_h = \sum_j^{N_h} u_j \varphi_j(x_1, x_2)$ fulfills the criteria,

$$\sum_{j=1}^{N_h} u_j a(\varphi_j, \varphi_i) = l(\varphi_i)$$

Hence, by letting $\mathbf{u} = [u_j]$, $\mathbf{f} = [(f, \varphi_i)_\Omega]$ and $A = [a(\varphi_j, \varphi_i)]$ can we construct a linear system,

$$A\mathbf{u} = \mathbf{f}.$$

Ultimately, we have the final linear system which can be solved for each unknown u_j.

[2] Some measure theorists might be upset for this informality.

3 Biharmonic Equation

3.1 Strong form of the Biharmonic Equation

Let $\Omega \subseteq \mathbb{R}^2$ be a bounded polygonal domain and $\partial\Omega$ be its corresponding boundary. Let the inhomogeneous fourth order biharmonic equation have the form,

$$\begin{aligned} \Delta^2 u + \alpha u &= f \quad \text{in } \Omega, \\ \partial_n u &= 0 \quad \text{on } \partial\Omega, \\ \partial_n \Delta u &= g(x) \quad \text{on } \partial\Omega. \end{aligned} \tag{5}$$

Here is $\Delta^2 = \Delta(\Delta)$ the biharmonic operator, also known as the bilaplacian. We will assume for the strong form that $u \in H^4(\Omega)$, α is a non-negative constant and $f \in L_2(\Omega)$. We may consider the functions $g(x)$ as a time independent boundary conditions. Such problems as (5) are often associated with the Cahn-Hilliard model [2] for phase separation. However, depending on how Cahn-Hilliard model is time discretized numerically can (5) naturally arise. We refer to [15] for more information on this.

3.2 Weak Form Biharmonic Equation in $H^4(\Omega)$

We want to introduce the full weak formulation of (5). Now, let the solution space be on the form,

$$V = \left\{ v \in H^2(\Omega) : \partial_n v = 0 \text{ on } \partial\Omega \right\}.$$

Let $u, v \in V$, then the derivation of the general weak form is,

$$\left(\Delta^2 u, v\right)_\Omega = \left(\partial_n \Delta u, v\right)_{\partial\Omega} - \left(\nabla(\Delta u), \nabla v\right)_\Omega$$

In fact, the simplest formulation has the form,

$$\left(\nabla(\Delta u), \nabla v\right)_\Omega = \left(\Delta u, \partial_n v\right)_{\partial\Omega} - \left(\Delta u, \Delta v\right)_\Omega,$$

A major issue with this formulation is that we do not have boundary condition for Δu. Instead, we can expand the term in the following fashion.

$$
\begin{aligned}
(\nabla(\Delta u), \nabla v)_\Omega &= \sum_{i=1}^{d} (\Delta \partial_{x_i} u, \partial_{x_i} v)_\Omega \\
&= \sum_{i=1}^{d} (\nabla \cdot (\nabla \partial_{x_i} u), \partial_{x_i} v)_\Omega \\
&= \sum_{i=1}^{d} (\partial_n \partial_{x_i} u, \nabla \partial_{x_i} v)_{\partial\Omega} - (\nabla \partial_{x_i} u, \nabla \partial_{x_i} v)_\Omega \\
&= (\partial_n \nabla u, \nabla v)_{\partial\Omega} - \left(D^2 u, D^2 v\right)_\Omega \\
&= (\partial_{nn} u, \partial_n v)_{\partial\Omega} + (\partial_{nt} u, \partial_t v)_{\partial\Omega} - \left(D^2 u, D^2 v\right)_\Omega .
\end{aligned}
$$

Hence, the boundary condition of Δu is integrated into the formulation. It can be denoted that D^2 is the Hessian matrix operator such that

$$
(D^2 u, D^2 v)_\Omega = \int_\Omega D^2 u : D^2 v dx,
$$

where $D^2 u : D^2 v$ is the inner product and similarly for $\partial_{nn} u = n \cdot D^2 u \cdot n$. Thus, we now have a weak form identity,

$$
\left(\Delta^2 u, v\right)_\Omega = \left(D^2 u, D^2 v\right)_\Omega + (\partial_n \Delta u, v)_{\partial\Omega} - (\partial_{nn} u, \partial_n v)_{\partial\Omega} - (\partial_{nt} u, \partial_t v)_{\partial\Omega} . \tag{6}
$$

Using weak form identity (6) and the boundary conditions stated in the strong form (5) can we write

$$
\begin{aligned}
\left(\Delta^2 u, v\right)_\Omega &= \left(D^2 u, D^2 v\right)_\Omega + \underbrace{(\partial_n \Delta u, v)_{\partial\Omega}}_{=(g,v)_{\partial\Omega}} - \underbrace{(\partial_{nn} u, \partial_n v)_{\partial\Omega}}_{=0} - \underbrace{(\partial_{nt} u, \partial_t v)_{\partial\Omega}}_{=0} \\
&= \left(D^2 u, D^2 v\right)_\Omega + (g, v)_{\partial\Omega}
\end{aligned} . \tag{7}
$$

We can now formulate the full weak formulation by solving for $u \in V$ such that

$$
a(u, v) = F(v) \quad \forall v \in V, \tag{8}
$$

where

$$
\begin{aligned}
a(u, v)_\Omega &= \left(D^2 u, D^2 v\right)_\Omega + \alpha (u, v)_\Omega , \\
F(v)_\Omega &= (f, v)_\Omega - (g, v)_{\partial\Omega} .
\end{aligned} \tag{9}
$$

In fact, the solution is unique for $\alpha > 0$. However, for $\alpha = 0$ must we assume the solvability condition,

$$
\int_\Omega f dx = \int_{\partial\Omega} g ds.
$$

This condition easily arise when using the substitution $v = 1$ in (8). To handle this, can we extended the solution space

$$V^* = \begin{cases} V & \alpha > 0 \\ \left\{ v \in V : \int_\Omega v dx = 0 \right\} & \alpha = 0, \end{cases}$$

Thus, the unique solution in $v \in V^*$ belongs to $H^3(\Omega)$ and we get the following elliptic regularity estimate [16],

$$|u|_{H^3(\Omega)} \leq C_\Omega \left(\|f\|_{L_2(\Omega)} + (1 + \alpha^{\frac{1}{2}}) \cdot \|w\|_{H^4(\Omega)} \right), \quad w \in H^4(\Omega).$$

4 Continuous Interior Penalty Method

4.1 Introduction

To solve (5) numerically do we want to introduce the continuous interior penalty method (CIP), which is a discontinuous Galerkin method (DG) using C^0 finite elements. There is several reasons why we want to apply nonconformal C^0 instead of the often used conformal C^1 finite elements for fourth order problems.

However, it is known that H^2 conforming methods requires global C^1 continuity [19], and creates difficulties creating elements which conserves this property. Some examples is the Argyris element, but it has been shown to be fairly complicated because you have to construct 21 degrees of freedom for triangle elements [10, 11]. However, some sources tend to say that this method outperforms traditional C^0 methods [20], but it still seems to be rarely applied. Nevertheless, it has also been shown DG methods that is conform and has no penalty terms that does converge [19]. Hence, makes the method simpler since it does not involve tuning of penalty parameters, thus might be promising. None of these conform methods mentioned has shown to retain the same properties in 3D.

For the CIP case is C^0 finite elements much simpler than obtaining C^1 finite elements. Also, compared to other similar methods such as the mixed finite element method, CIP does in fact preserve the symmetric positive definiteness, which means the stability analysis is more straight forward. Finally and most importantly, according to [15] can naive use mixed methods of splitting the boundary conditions of the problem (5) produce wrong solutions if Ω is non convex.

4.2 Computational Domains

Let $\mathcal{T} = \{T\}$ be a triangulation of $\Omega \subset \mathbb{R}^2$ consisting of triangles T. We may also define the set of all facets $\mathcal{F}_h$, where every facet is denoted by $F \in \mathcal{F}_h$. However, we will distinguish between the set of external facets $\mathcal{F}_h^{ext}$, which is all facets along $\partial\Omega$, and the interior facets $\mathcal{F}_h^{int}$. Let the facets be denotes as $F \in \mathcal{F}_h$, then the normal vector n is across the facets from T^+ to T^-, illustrated in figure 1.

A parameter which is useful is the maximum diameter h of the set of triangles $\{T\}$, which we to be defined such that,

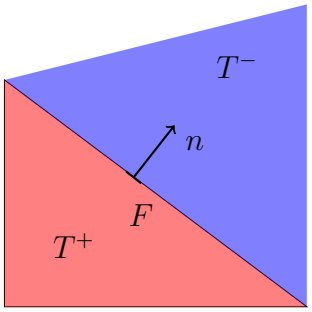

Figure 1: Facet $F \in \mathcal{F}_h$ shared by the triangles $T^+, T^- \in \mathcal{T}_h$ and the normal unit vector n.

$$\begin{aligned} h_T &= diam\,(T) = \max_{x_1,x_2 \in T} dist(x_1, x_2), \\ h_{min} &= \min_{T \in \mathcal{T}} h_T, \\ h_{max} &= \max_{T \in \mathcal{T}} h_T := h, \end{aligned} \qquad . \tag{10}$$

where the $diam(T)$ is the largest facet for a triangle T. We will also assume mesh conform i.e., if $T_1 \neq T_2$ and $T \cap T_2 \neq \emptyset$, then they share either a vertex or a facet.

Let the chunkiness parameter $c_T := h_T/r_T$, where r_T is the largest ball that be inscribed inside the element T. We can then assume that the mesh is shape regular, i.e., that $c_T \leq c$ independent of T and h. We may also assuming that the mesh is quasi-uniform only if it holds that the mesh is shape regular and $h_{max} \leq c h_{min}$.

4.3 Constructing Continuous Interior Penalty Method

Let us assume that $u, v \in H^4\,(T)$. Using that the weak form identity (6) also holds for a triangle T can we write

$$\left(\Delta^2 u, v\right)_T = \left(D^2 u, D^2 v\right)_T - \left(\partial_{nt} u, \partial_t v\right)_{\partial T} - \left(\partial_{nn} u, \partial_n v\right)_{\partial T} + \left(\partial_n \Delta u, v\right)_{\partial T}. \tag{11}$$

For global continuity, let $v \in V = \{v \in H^1\,(\Omega) : v_T \in H^4\,(T)\,,\ \forall T \in \mathcal{T}_h\}$ and $u \in H^4\,(\Omega)$ such that,

$$\left(\Delta^2 u, v\right)_\Omega = \sum_{T \in \mathcal{T}_h} \left(D^2 u, D^2 v\right)_T - \left(\partial_{nt} u, \partial_t v\right)_{\partial T} - \left(\partial_{nn} u, \partial_n v\right)_{\partial T} + \left(\partial_n \Delta u, v\right)_{\partial T}. \tag{12}$$

However, this expression can be written to distinguish integrating over triangles $\mathcal{T}_h$, integrating over exterior facets $\mathcal{F}_h^{ext}$ and then integrate interior facets $\mathcal{F}_h^{int}$.

$$
\begin{aligned}
\left(\Delta^2 u, v\right)_\Omega &= \sum_{T\in\mathcal{T}_h} \left(D^2 u, D^2 v\right)_T \\
&\quad + \sum_{F\in\mathcal{F}_h^{ext}} \left(\partial_n \Delta u, v\right)_F - \left(\partial_{nt} u, \partial_t v\right)_F - \left(\partial_{nn} u, \partial_n v\right)_F \\
&\quad + \sum_{F\in\mathcal{F}_h^{int}} \left(\partial_{nn} u, [\![\partial_n v]\!]\right)_F \\
&= \sum_{T\in\mathcal{T}_h} \left(D^2 u, D^2 v\right)_T + \sum_{F\in\mathcal{F}_h^{ext}} \left(g, v\right)_F + \sum_{F\in\mathcal{F}^{int}} \left(\partial_{nn} u, [\![\partial_n v]\!]\right)_F
\end{aligned}
\tag{13}
$$

Keep in mind that any jump over a interior facet $F \subset \mathcal{F}_h^{int}$, visualized in figure 1, is defined as $[\![a]\!] = a^+ - a^-$ and likewise for the mean, $\{\!\{a\}\!\} = \frac{1}{2}(a^+ + a^-)$. The equivalence of (12) and (13) comes from the following argumentation.

$$
\begin{aligned}
\left(\Delta^2 u, v\right)_\Omega &= \sum_{T\in\mathcal{T}_h} \left(D^2 u, D^2 v\right)_T - \left(\partial_{nt} u, \partial_t v\right)_{\partial T} - \left(\partial_{nn} u, \partial_n v\right)_{\partial T} + \left(\partial_n \Delta u, v\right)_{\partial T} \\
&= \sum_{T\in\mathcal{T}_h} \left(D^2 u, D^2 v\right)_T \\
&\quad + \sum_{F\in\mathcal{F}_h^{ext}} \underbrace{\left(\partial_n \Delta u, v\right)_F}_{=(g,v)_F} - \left(\partial_{nt} u, \partial_t v\right)_F - \underbrace{\left(\partial_{nn} u, \partial_n v\right)_F}_{=0} \\
&\quad + \sum_{F\in\mathcal{F}_h^{int}} \underbrace{\left(\left(\partial_{n^+} \Delta u^+, v^+\right)_F + \left(\partial_{n^-} \Delta u^+, v^-\right)_F\right)}_{(I)} \\
&\qquad + \underbrace{\left(\left(\partial_{n^+ t} u^+, \partial_t v^+\right)_F + \left(\partial_{n^- t} u^-, \partial_t v^-\right)_F\right)}_{(II)} \\
&\qquad + \underbrace{\left(\left(\partial_{n^+ n^+} u^+, v^+\right)_F + \left(\partial_{n^- n^-} u^-, v^-\right)_F\right)}_{(III)}
\end{aligned}
$$

Where integration over all interior facets $\forall F \in \mathcal{F}_h^{int}$ is computed in this way.

$$
\begin{aligned}
(I) &= \left(\partial_{n^+}\Delta u^+, v^+\right)_F + \left(\partial_{n^-}\Delta u^+, v^-\right)_F \\
&= \int_F [\![\partial_n \Delta u \cdot v]\!] = \int_F \{\!\{\partial_n \Delta u\}\!\} \underbrace{[\![v]\!]}_{=0} + \underbrace{[\![\partial_n \Delta u]\!]}_{=0} \{\!\{v\}\!\} = 0 \\
(II) &= \left(\partial_{n^+t} u^+, \partial_t v^+\right)_F + \left(\partial_{n^-t} u^-, \partial_t v^-\right)_F \\
&= \int_F [\![\partial_{nt} u \cdot \partial_t v]\!] = \int_F \{\!\{\partial_{nt} u\}\!\} \underbrace{[\![\partial_t v]\!]}_{=0} + \underbrace{[\![\partial_{nt} u]\!]}_{=0} \{\!\{\partial_t v\}\!\} = 0 \\
(III) &= \left(\partial_{n^+n^+} u^+, \partial_{n^+} v^+\right)_F + \left(\partial_{n^-n^-} u^-, \partial_{n^-} v^-\right)_F = \int_F [\![\partial_{nn} u \cdot \partial_n v]\!] \\
&= \int_F \{\!\{\partial_{nn} u\}\!\} \underbrace{[\![\partial_n v]\!]}_{\neq 0} + \underbrace{[\![\partial_{nn} u]\!]}_{=0} \{\!\{\partial_n v\}\!\} = \left(\partial_{nn} u, [\![\partial_n v]\!]\right)_F
\end{aligned}
$$

Observe that the cancellations in the term (I) appears of the continuity of $v \in V$ and $u \in H^4(\Omega)$ which makes the jumps zero. For the second term (II) does the terms become zero cancelled because the tangential derivative at the facet has no jump. However, The third term (III) is fairly interesting since the discontinuity in normal vector for $v \in V$ is a jump, while the second term is still continuous. It can also be raised that $\{\!\{\partial_{nn} u\}\!\} = \partial_{nn} u$ holds by the continuity of $H^4(\Omega)$. Anyhow, the definition of jump of should more interesting when we later weaken the continuity of u during discretization. Hence, (12) and (13) is equivalent.

4.4 Formulation of Continious Interior Penalty Method

We can finally start defining the fully discrete formulation. Let the basis be a $\mathcal{P}_2$ Lagrange finite element space so,

$$V_h = \left\{v \in C^0(\Omega) : v_T = v|_T \in \mathcal{P}_2(T), \forall T \in \mathcal{T}_h\right\}$$

and

$$V_h^* = \begin{cases} V_h & \text{if } \alpha > 0 \\ \left\{v \in V_h : \int_\Omega v dx = 0\right\} & \text{if } \alpha = 0 \end{cases}$$

Now, if we choose $u \in V_h$ must we take account that the jump is discrete. We have now the final CIP formulation. The discretized numerical problem is to solve $w_h \in V_h^*$ such that

$$\mathcal{A}(w_h, v_h) = F(v_h), \quad \forall v_h \in V_h^*. \tag{14}$$

where

$$\begin{aligned}\mathcal{A}(w_h, v_h) = \quad & (\alpha w_h, v_h)_\Omega \\ & + \sum_{T\in\mathcal{T}_h} \left(D^2 w_h, D^2 v_h\right)_T \\ & + \sum_{F\in\mathcal{F}_h^{int}} \left(\{\!\{\partial_{nn} w_h\}\!\}, [\![\partial_n v_h]\!]\right)_F + \left(\{\!\{\partial_{nn} v_h\}\!\}, [\![\partial_n w]\!]\right)_F \\ & \qquad + \frac{\gamma}{h}\left([\![\partial_n w_h]\!], [\![\partial_n v_h]\!]\right)_F\end{aligned} \tag{15}$$

and

$$F(v_h) = (f, v_h)_\Omega + \sum_{F\in\mathcal{F}_h^{ext}} -(g, v_h)_F . \tag{16}$$

Notice that the regulation term determined by respectively a global tuning parameter $\gamma > 0$. Another key component to the formulation in (15) after introduction of $w_h, v_h \in V_h^*$ is that we expanded $(\partial_{nn} w, [\![\partial_n v]\!])_F \to (\{\!\{\partial_{nn} w_h\}\!\}, [\![\partial_n v_h]\!])_F$ since we can longer not guarantee a continuous jump. For symmetric purposes we also added $(\{\!\{\partial_{nn} v_h\}\!\}, [\![\partial_n w_h]\!])_F$. For convenience will we introduce the compact notation of (15),

$$\begin{aligned}\mathcal{A}(w_h, v_h) = \quad & (\alpha w_h, v_h)_\Omega \\ & + \left(D^2 w_h, D^2 v_h\right)_{\mathcal{T}_h} \\ & + \left(\{\!\{\partial_{nn} w_h\}\!\}, [\![\partial_n v_h]\!]\right)_{\mathcal{F}_h} + \left(\{\!\{\partial_{nn} v_h\}\!\}, [\![\partial_n w]\!]\right)_{\mathcal{F}_h} \\ & + \frac{\gamma}{h}\left([\![\partial_n w_h]\!], [\![\partial_n v_h]\!]\right)_{\mathcal{F}_h}\end{aligned} . \tag{17}$$

4.5 Stability Results

To guarantee convergence and stability we may want to check coercivity and boundedness of the method.

First of all, let us now establish some important inequalities.

$$\begin{aligned}\textbf{Cauchy-Schwarz inequality:}\quad & \|ab\| \le \|a\|\,\|b\| \\ \textbf{Inverse inequality:}\quad & \frac{1}{h}\|\partial_{nn} v_h\|^2_{\mathcal{F}_h} \le C_j \|D^2 v_h\|^2_{\mathcal{T}_h} \\ \textbf{Youngs epsilon inequality:}\quad & 2ab = 2\sqrt{\varepsilon}a \cdot \frac{b}{\sqrt{\varepsilon}} \le \varepsilon a^2 + b^2 \frac{1}{\varepsilon}\end{aligned}$$

Let the energy norm be on the form,

$$\begin{aligned}\|v_h\|_h^2 &= \|v_h\|_{a_h}^2 = \|v_h\|_\Omega^2 + \|D^2 v_h\|_{\mathcal{T}_h}^2 + \|h^{-\frac{1}{2}}[\![\partial_n v_h]\!]\|_{\mathcal{F}_h}^2, \\ \|v\|_h^2 &= \|v\|_{a_h,*}^2 = \|v\|_{a_h}^2 + \|h^{\frac{1}{2}}\{\partial_{nn} v\}\|_{\mathcal{F}_h}^2, \quad v \in V \oplus V_h.\end{aligned} \tag{18}$$

The method is said to be coercive if $\mathcal{A}_h(v_h, v_h) \geq C\|v_h\|_{a_h}$. Similarly, it is bounded if $\mathcal{A}_h(v_h, u_h) \leq C\|u_h\|_{a_h}^2\|v_h\|_{a_h}^2$ and then, according to Lax Milgram the problem is said to be well posed.

4.5.1 Coercivity

Suppose we have the CIP problem described in (14). Then is the coercivity be computed such that,

$$
\begin{aligned}
\mathcal{A}(v_h, v_h) = \;& \alpha\|v_h v_h\|_\Omega + \|D^2 v_h\|_{\mathcal{T}_h}^2 \\
& + 2\left(\{\!\{\partial_{nn} v_h\}\!\}, [\![\partial_n v_h]\!]\right)_{\mathcal{F}_h} + \frac{\gamma}{h}\|[\![\partial_n v_h]\!]\|_{\mathcal{F}_h}^2 \\
\textit{Cauchy-Schwarz inequality} \quad \geq \;& \alpha\|v_h\|_\Omega\|v_h\|_\Omega + \|D^2 v_h\|_{\mathcal{T}_h}^2 \\
& - 2\|h^{\frac{1}{2}}\{\!\{\partial_{nn} v_h\}\!\}\|_{\mathcal{F}_h}\|h^{-\frac{1}{2}}[\![\partial_n v_h]\!]\|_{\mathcal{F}_h} + \gamma\|h^{-\frac{1}{2}}[\![\partial_n v_h]\!]\|_{\mathcal{F}_h}^2 \\
\textit{Inverse inequality} \quad \geq \;& \alpha\|v_h\|_\Omega\|v_h\|_\Omega + \|D^2 v_h\|_{\mathcal{T}_h}^2 \\
& - 2C_j^{\frac{1}{2}}\|D^2 v_h\|_{\mathcal{T}_h}\|h^{-\frac{1}{2}}[\![\partial_n v_h]\!]\|_{\mathcal{F}_h} + \gamma\|h^{-\frac{1}{2}}[\![\partial_n v_h]\!]\|_{\mathcal{F}_h}^2 \\
\textit{Youngs epsilon inequality} \quad \geq \;& \alpha\|v_h\|_\Omega\|v_h\|_\Omega + \|D^2 v_h\|_{\mathcal{T}_h}^2 - \varepsilon C_j\|D^2 v_h\|_{\mathcal{T}_h}^2 \\
& - \frac{1}{\varepsilon}\|h^{\frac{1}{2}}[\![\partial_n v_h]\!]\|_{\mathcal{F}_h}^2 + \gamma\|h^{-\frac{1}{2}}[\![\partial_n v_h]\!]\|_{\mathcal{F}_h}^2 \\
= \;& \alpha\|v_h\|_\Omega\|v_h\|_\Omega + (1 - \varepsilon C_j)\|D^2 v_h\|_{\mathcal{T}_h}^2 \\
& + \left(\gamma - \frac{1}{\varepsilon}\right)\|h^{-\frac{1}{2}}[\![\partial_n v_h]\!]\|_{\mathcal{T}_h}^2 \\
(\varepsilon = \frac{1}{2C_j}) \implies \quad = \;& \alpha\|v_h\|_\Omega\|v_h\|_\Omega + \frac{1}{2}\|D^2 v_h\|_{\mathcal{T}_h}^2 + \underbrace{(\gamma - 2C_j)}_{\geq \frac{1}{2}}\|h^{\frac{1}{2}}[\![\partial_n v_h]\!]\|_{\mathcal{F}_h}^2 \\
\geq \;& C\|v_h\|_{a_h}^2
\end{aligned}
$$

This holds if $C = \min\{\alpha, 1/2\}$. Observe that for the first inequality is the standard **Cauchy-Schwarz inequality** such that

$$
\left(\{\!\{\partial_{nn} v_h\}\!\}, [\![\partial_n v_h]\!]\right)_{\mathcal{F}_h} \geq -\|h^{-\frac{1}{2}}\{\!\{\partial_{nn} v_h\}\!\}\|_{\mathcal{F}_h}\|\{\!\{\partial_n v_h\}\!\}\|_{\mathcal{F}_h}.
$$

On the second inequality the **Inverse inequality** was applied,

$$
-\|h^{\frac{1}{2}}\{\!\{\partial_{nn} v\}\!\}\|_{\mathcal{F}_h} \geq -C_j^{\frac{1}{2}}\|D^2 v_h\|_{\mathcal{T}_h}
$$

The next step is then to use the **Youngs epsilon inequality** to separate the facets and triangulation norms,

$$
-2C_j^{\frac{1}{2}}\|D^2 v_h\|_{\mathcal{T}_h}\|h^{\frac{1}{2}}[\![\partial_n v_h]\!]\|_{\mathcal{F}_h} \geq -\varepsilon C_j\|D^2 v_h\|_{\mathcal{T}_h}^2 - \frac{1}{\varepsilon}\|h^{\frac{1}{2}}[\![\partial_n v_h]\!]\|_{\mathcal{F}_h}^2.
$$

The last step was to choose a ε and γ as some positive constant so that the second term is restricted to be multiplied with something bigger than $\frac{1}{2}$. Thus, the term fulfils coercivity of the (18). Hence, the CIP method is coercive.

4.5.2 Boundedness

We want the CIP method to be bounded.

$$
\begin{aligned}
\mathcal{A}(w_h, v_h) = \quad & (\alpha w_h, v_h)_\Omega + \left(D^2 w_h, D^2 v_h\right)_{\mathcal{T}_h} \\
& + \left(\{\!\{\partial_{nn} w_h\}\!\}, [\![\partial_n v_h]\!]\right)_{\mathcal{F}_h} + \left(\{\!\{\partial_{nn} v_h\}\!\}, [\![\partial_n w]\!]\right)_{\mathcal{F}_h} \\
& + \frac{\gamma}{h}\left([\![\partial_n w_h]\!], [\![\partial_n v_h]\!]\right)_{\mathcal{F}_h} \\
\textit{Cauchy-Schwarz inequality} \quad \leq \quad & \alpha \|w_h\|_\Omega \|v_h\|_\Omega + \|D^2 w_h\|_{\mathcal{T}_h} \|D^2 v_h\|_{\mathcal{T}_h} \\
& + \|h^{\frac{1}{2}} \{\!\{\partial_{nn} w_h\}\!\}\|_{\mathcal{F}_h} \|h^{-\frac{1}{2}} [\![\partial_n v_h]\!]\|_{\mathcal{F}_h} \\
& + \|h^{\frac{1}{2}} \{\!\{\partial_{nn} v_h\}\!\}\|_{\mathcal{F}_h} \|h^{-\frac{1}{2}} [\![\partial_n w_h]\!]\|_{\mathcal{F}_h} \\
& + \gamma \|h^{-1} [\![\partial_n v_h]\!]\|_{\mathcal{F}_h} \|[\![\partial_n w_h]\!]\|_{\mathcal{F}_h} \\
\textit{Inverse inequality} \quad \leq \quad & \alpha \|w_h\|_\Omega \|v_h\|_\Omega + \|D^2 w_h\|_{\mathcal{T}_h} \|D^2 v_h\|_{\mathcal{T}_h} \\
& + C_j^{\frac{1}{2}} \|D^2 w_h\|_{\mathcal{T}_h} \|h^{-\frac{1}{2}} [\![\partial_n v_h]\!]\|_{\mathcal{F}_h} \\
& + C_j^{\frac{1}{2}} \|D^2 w_h\|_{\mathcal{T}_h} \|h^{-\frac{1}{2}} [\![\partial_n w_h]\!]\|_{\mathcal{F}_h} \\
& + \gamma \|h^{-1} [\![\partial_n v_h]\!]\|_{\mathcal{F}_h} \|[\![\partial_n w_h]\!]\|_{\mathcal{F}_h} \\
\textit{Using (19)} \quad \leq \quad & \alpha \|w_h\|_{a_h} \|v_h\|_{a_h} + \|w_h\|_{a_h} \|v_h\|_{a_h} + 2C_j^{\frac{1}{2}} \|w_h\|_{a_h} \|v_h\|_{a_h} \\
& + \gamma \|v_h\|_{a_h} \|w_h\|_{a_h} \\
\leq \quad & \left(\alpha + 1 + 2C_j^{\frac{1}{2}} + \gamma\right) \|v_h\|_{a_h} \|w_h\|_{a_h} \leq K \|v_h\|_{a_h} \|w_h\|_{a_h}
\end{aligned}
$$

Thus, the CIP method is shown to be bounded. Again, the first step was to apply the **Cauchy-Schwarz inequality** for every term. On the second inequality the **Inverse inequality** was applied so that

$$
\|h^{\frac{1}{2}} \{\!\{\partial_{nn} v_h\}\!\}\|_{\mathcal{F}_h} \leq C_j^{\frac{1}{2}} \|D^2 v_h\|_{\mathcal{T}_h} \quad \text{and} \quad \|h^{\frac{1}{2}} \{\!\{\partial_{nn} w_h\}\!\}\|_{\mathcal{F}_h} \leq C_j^{\frac{1}{2}} \|D^2 w_h\|_{\mathcal{T}_h}.
$$

The second step can we luckily observe that all terms invidually is less than the norm, that is,

$$
\begin{aligned}
\|w_h\|_\Omega \|v_h\|_\Omega &\leq \|w_h\|_{a_h} \|v_h\|_{a_h}, \\
\|D^2 w_h\|_{\mathcal{T}_h} \|D^2 v_h\|_{\mathcal{T}_h} &\leq \|w_h\|_{a_h} \|v_h\|_{a_h}, \\
\|D^2 w_h\|_{\mathcal{T}_h} \|h^{-\frac{1}{2}} [\![\partial_n v_h]\!] \|_{\mathcal{F}_h} &\leq \|w_h\|_{a_h} \|v_h\|_{a_h}, \\
\|D^2 v_h\|_{\mathcal{T}_h} \|h^{-\frac{1}{2}} [\![\partial_n w_h]\!] \|_{\mathcal{F}_h} &\leq \|w_h\|_{a_h} \|v_h\|_{a_h}, \\
\gamma \|h^{-1} [\![\partial_n v_h]\!] \|_{\mathcal{F}_h} \| [\![\partial_n w_h]\!] \|_{\mathcal{F}_h} &\leq \gamma \|w_h\|_{a_h} \|v_h\|_{a_h}.
\end{aligned} \tag{19}
$$

Hence, the CIP method is does fulfills the Lax Milgram criteria because it is both bounded and unique.

4.6 Interpolations Estimates

We want to compute the expected convergence rate of the energy norm (18). An important tool in the process is the Cléments interpolation operator, C_h. It is used for interpolation on non smooth functions and is defined as a local L^2 projection onto the so-called macroelements, that is, $C_h : H^m(\Omega) \mapsto V_h$. For further detailed information, please investigate [21].

Recall the definition (1) and let us define the integral norm notation,

$$
\|u\|_{m,2,T} = \left(\sum_{|\alpha| \leq m} \int_T |\partial^\alpha u|^2 \, dx \right)^{\frac{1}{2}}
$$

We denote a patch, $\omega(T)$, as the set of elements in $\mathcal{T}_h$ sharing at least one vertex with $T \in \mathcal{T}_h$. And similarly we denote a another patch, $\omega(F)$, as the set of all elements in $\mathcal{T}_h$ sharing at least one vertex with $F \in \mathcal{F}_h$. Furthermore, we also introduce the notation ∂T for integration along the facets for a triangle T.

Now, let the interpolation estimate have the form $u - C_h u$. The stability and interpolation properties of the Cléments interpolation operator has proven to be useful. In fact, Cléments lemma says that the operator satisfies [21],

$$
\|C_h v\|_{H^m(\Omega)} \lesssim \|v\|_{H^m(\Omega)} \quad \forall v \in H^m(\Omega),
$$

and if the following conditions for m, l and k is satisfied, it exists error estimates such that,

$$
\begin{aligned}
m \leq l \leq k+1 &\implies \|v - C_h v\|_{m,2,T} \lesssim h_T^{l-m} \|v\|_{l,2,\omega(T)} \quad \forall T \in \mathcal{T}_h, \forall v \in H^l(\omega(T)), \\
m + \frac{1}{2} \leq l \leq k+1 &\implies \|v - C_h v\|_{m,2,F} \lesssim h_T^{l-m-\frac{1}{2}} \|v\|_{l,2,\omega(F)} \quad \forall \partial T \in \mathcal{T}_h, \forall v \in H^l(\omega(F)).
\end{aligned}
$$

We will use these estimates to compute convergence rate.

Firstly and foremost, let the energy norm error be formulated as,

$$\|u - C_h u\|_{a_h,*}^2 = \underbrace{\|D^2(u - C_h u)\|_\Omega^2}_{(I)} + \gamma \underbrace{\|h^{-\frac{1}{2}} [\![\partial_n (u - C_h u)]\!] \|_{\mathcal{F}_h}^2}_{(II)} + \underbrace{\alpha^2 \|u - C_h u\|_\Omega^2}_{(III)} + \underbrace{\|h^{\frac{1}{2}} \{\!\{\partial_{nn} (u - C_h u)\}\!\} \|_{\mathcal{F}_h}^2}_{(IV)}.$$

Observe that by summing over triangles the jump and mean terms (respectively term II and IV) is notable simplified,

$$\sum_{F \in \mathcal{F}_h} \| [\![v]\!] \|_F = \sum_{F \in \mathcal{F}_h} \|v^+ - v^-\|_F \leq \sum_{F \in \mathcal{F}_h} \|v^+\|_F + \|v^-\|_F \leq \sum_{T \in \mathcal{T}_h} \|v\|_{\partial T}$$
$$\sum_{F \in \mathcal{F}_h} \| \{\!\{v\}\!\} \|_F = \sum_{F \in \mathcal{F}_h} \frac{1}{2}\|v^+ + v^-\|_F \leq \sum_{F \in \mathcal{F}_h} \frac{1}{2}\|v^+\|_F + \frac{1}{2}\|v^-\|_F \leq \sum_{T \in \mathcal{T}_h} \|v\|_{\partial T}.$$

Using this fact and applying Cléments lemma we get,

$$\begin{aligned}
(I) &\leq \|D^2 (u - C_h u)\|_{\mathcal{T}_h}^2 = \sum_{T \in \mathcal{T}_h} \|D^2 (u - C_h u)\|_T^2 \\
&\lesssim \sum_{T \in \mathcal{T}_h} \|(u - C_h u)\|_{2,T}^2 \lesssim \sum_{T \in \mathcal{T}_h} h_T^{2(l-2)} \|u\|_{l,\omega(T)}^2, \\
(II) &\leq \sum_{T \in \mathcal{T}_h} h^{-1} \|\partial_n (u - C_h)\|_{\partial T} \leq \sum_{T \in \mathcal{T}_h} h^{-1} \left(h^{l-1-\frac{1}{2}} \|u\|_{l,\omega(T)} \right)^2, \\
&\lesssim \sum_{T \in \mathcal{T}_h} h^{2(l-2)} \|u\|_{l,\omega(F)}^2 \\
(III) &\leq \alpha^2 \sum_{T \in \mathcal{T}_h} \|u - C_h\|_T^2 \lesssim \sum_{T \in \mathcal{T}_h} h^{2l} \|u\|_{\omega(T)}^2, \\
(IV) &\leq \sum_{T \in \mathcal{T}_h} h \|\partial_{nn} (u - C_h)\|_{\partial T}^2 \lesssim \sum_{T \in \mathcal{T}_h} h \left(h^{l-2-\frac{1}{2}} \|u\|_{l,\omega(F)} \right)^2 \lesssim \sum_{T \in \mathcal{T}_h} h^{2(l-2)} \|u\|_{l,\omega(F)}^2.
\end{aligned}$$

The result then follows easily,

$$\begin{aligned}
(I) + (II) + (III) + (IV) &\lesssim \sum_{T \in \mathcal{T}_h} h_T^{2(l-2)} \|u\|_{l,\omega(T)} + 2 \cdot h^{2(l-2)} \|u\|_{l,\omega(F)}^2 + h_T^{2l} \|u\|_{l,\omega(T)} \\
&\lesssim h^{2(l-2)} \|u\|_{H^l(\Omega)}^2.
\end{aligned}$$

Ergo, we now have a convergence rate estimate,

$$\|u - C_h u\|_{a_h,*} \lesssim h^{l(l-2)} \|u\|_{H^l(\Omega)}.$$

It is easy to that we must require u to be at least be in $H^3(\Omega)$ since,

$$u \in H^3(\Omega) \implies \begin{cases} \Delta u \in H^1(\Omega) \\ \nabla u \in H^2(\Omega), \partial_n u \in H^{\frac{3}{2}}(\Gamma) \\ D^2 u \in H^1(\Omega), \quad \partial_{nn} u \in H^{\frac{1}{2}}(\Gamma) \end{cases}.$$

Thus, if we let $u_h \in \mathcal{P}^k$ and $u \in H^l(\Omega)$, then a reasonable assumption is that $3 \leq l \leq k+1$.

4.7 A Priori Estimates

We will now introduce the notion of an a priori estimate, which can be used the estimate the size of a solution even before we have a solution. Since we have discrete coercivity, then $V_h \not\subseteq V$, thus the standard method does not work. Firstly, we want to use the results from 4.5. We have shown that

$$\begin{aligned} &\textit{Discrete coercivity} && \hat{\alpha}\|u_h\|_{a_h}^2 \leq \mathcal{A}(u_h, u_h) \\ &\textit{Boundedness (semi-discrete)} && \mathcal{A}(v, w_h) \leq \widetilde{C}\|v\|_{a_{h,*}}\|w_h\|_{a_h} \quad \forall v \in V_h \oplus H^4(\Omega). \\ &\textit{Boundedness (fully discrete)} && \mathcal{A}(v_h, w_h) \leq \overline{C}\|v\|_{a_{h,*}}\|w_h\|_{a_h} \quad \forall v_h, w_h \in V_h \end{aligned}$$

Let the difference have the form $u - u_h = (u - v_h) + (v_h - u_h)$ and the define identity,

$$\|w_h\|_{a_{h,*}} \leq D\|w_h\|_{a_h}, \forall w_h \in V_h.$$

Thus, the norm can now be computed such that,

$$\|u - u_h\|_{a_{h,*}} \leq \|u - v_h\|_{a_{h,*}} + \|v_h - u_h\|_{a_{h,*}} \leq \|u - v_h\|_{a_{h,*}} + D\|u_h - v_h\|_{a_h}.$$

Finally, following the same procedure as in (4) we get,

$$\begin{aligned} \|u_h - v_h\|_{a_h}^2 \hat{\alpha} &\leq \mathcal{A}(u_h - v_h, u_h - v_h) \\ &= \mathcal{A}_h(u_h - u, u_h - v_h) + \mathcal{A}(u - v_h, u_h - v_h) \\ &\leq \mathcal{A}(u - v_h, u_h - v_h) \\ &\leq \widetilde{C}\|u - v_h\|_{a_{h,*}}\|u - v_h\|_{a_h}. \end{aligned}$$

Observe that we now have $\|u_h - v_h\|_{a_h} \leq \frac{\widetilde{C}}{\hat{\alpha}}\|u - v_h\|_{a_{h,*}}$ and $\|u - u_h\|_{a_{h,*}} \leq \left(1 + D\widetilde{C}/\hat{\alpha}\right) \cdot \|u - v_h\|_{a_{h,*}}$. Hence, we have derived a equivalent Céa's lemma for

the CIP method.

$$\|u_h - v_h\|_{a_h} \leq \frac{\widetilde{C}}{\hat{\alpha}} \inf_{v_h \in V_h} \|v_h - u\|_{a_{h,*}}$$
$$\|u - u_h\|_{a_{h,*}} \leq \left(1 + D\widetilde{C}/\hat{\alpha}\right) \cdot \inf_{v_h \in V_h} \|u - v_h\|_{a_{h,*}}$$

By combing Cléments lemma and Céa's lemma can we now, in fact, conclude that the energy norm has the convergence rate estimate,

$$\|u - u_h\|_{a_{h,*}} \lesssim h^{k-1}. \tag{20}$$

5 Numerical Experiments

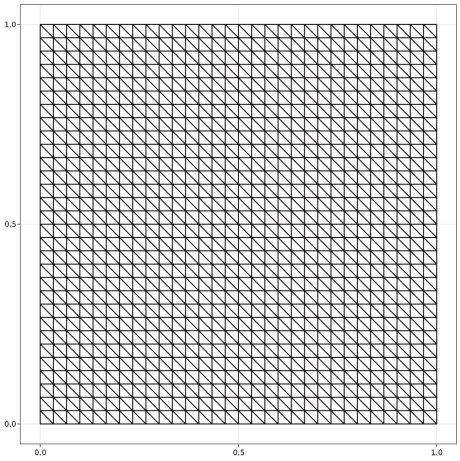

Figure 2: Example of mesh on $\Omega = (0, L)^2$ where $h = \frac{L}{16}$ for $L = 1$

All numerical experiments were carried out on a square with side length L. The convergence analysis were performed for polynomial basis, $\mathcal{P}_k$, with order $k = 2, 3, 4$, and a sequence of triangulations, $\mathcal{T}_{h_i}$, for $h_i = \frac{L}{4} \cdot 2^{-i}$ where $i = 0, \ldots, 5$. An illustration of the triangulation can be seen on figure 2.

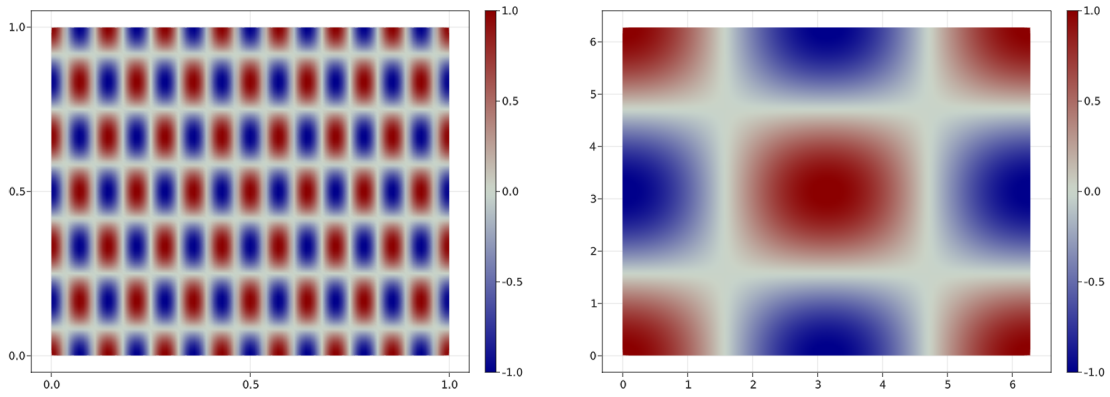

(a) (b)

Figure 3: The manufactured solution (21) with the model parameters $L = 1$, $m = 7$ and $r = 3$ in $\Omega = (0, 1)^2$ illustrated in 3a and similarly, $L = 2\pi$, $m = 1$ and $r = 1$ in $\Omega = (0, 2\pi)^2$ illustrated in 3b

We choose the manufactured solutions to be on the form,

$$u\left(x; L, m, r\right) = \cos\left(m \cdot \frac{2\pi}{L} x_1\right) \cos\left(r \cdot \frac{2\pi}{L} x_2\right) \quad \text{on } \Omega = (0, L)^2 . \tag{21}$$

Notice that we customize the model parameters L, m and r freely. For convenience did we pick $\alpha = 1$ in all the numerical experiments. We define the error to have the form $e = u - u_h$ such that the L^2 norm is denoted as $\|e\|_{L^2(\Omega)}$, its H^1 norm is denoted as $\|e\|_{H^1(\Omega)}$ and the energy norm (18) denoted as $\|e\|_{a_h,*}$. In this report will we provide two examples of convergence analysis based on different parametrization of (21). Each examples consists of a convergence plot of different penalty parameters γ using the L^2 norm and a more extensive analysis by comparing the convergence rate of their respective norms. A convenient tool to measure convergence is by computing the experimentally observed convergence rate (EOC), defined as follows,

$$EOC(i) = \frac{\log\left(\frac{\|e(h_i)\|_{\mathcal{V}}}{\|e(h_{i-1})\|_{\mathcal{V}}}\right)}{\log\left(\frac{h_i}{h_{i-1}}\right)}, \quad i = 1, \ldots, 5.$$

The FEM software package used in the implementation was Gridap written in the Julia programming language [22, 23].

The first example, where $L = 1$, $m = 7$ and $r = 3$, (illustrated on figure 3a) with a penalty parameter analysis on figure 4 and a extensive convergence analysis on figures 5a, 5b and 5c with corresponding tables 1, 2 and 3. Similarly, the second example, where $L = 2\pi$, $m = 1$ and $r = 1$, (illustrated on figure 3b) with a penalty parameter analysis on figure 6 and a extensive convergence analysis on figures 7a, 7b and 7c with corresponding tables 4, 5 and 6.

Generally speaking, for both examples do we observe that the convergence rate is robust for most choices of γ for any order. However, we can also observe in both cases some numerical instabilities for order $k = 4$ and $h = \frac{1}{128}$. The cause is likely because of a ill conditioned linear system. In fact, it has been shown that the condition number has a growth rate of $O\left(h^{-4}\right)$ [24], so this behaviour is expected without preconditioning of the linear system.

Observing the convergence rate can we see in both examples that the theoretical estimate for the energy norm (20) matches the observed EOC. Furthermore, the we can see that the EOC is affected by the numerical instability discussed above. Likewise, it has been shown that the L^2 norm, while not presented in this report, has the expected the theoretical estimates [25],

$$\|u - u_h\|_\Omega \lesssim O\left(h^k\right), \quad k = 2$$
$$\|u - u_h\|_\Omega \lesssim O\left(h^{k+1}\right), \quad k \geq 3.$$

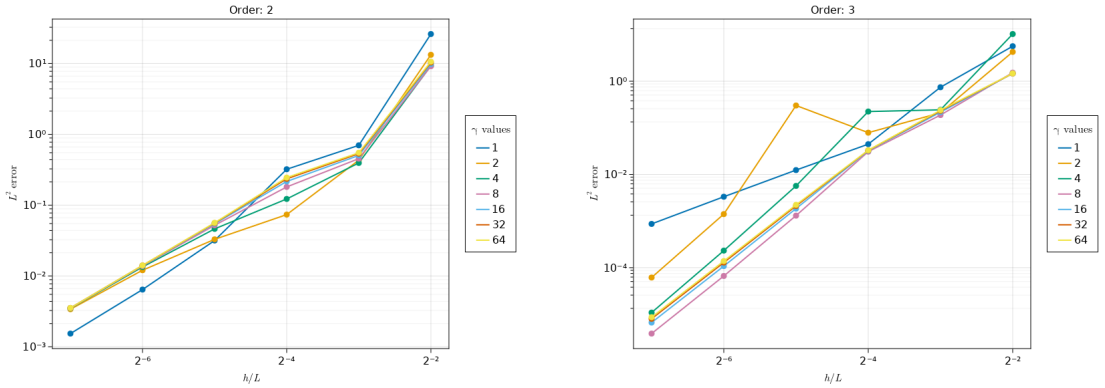

(a) (b)

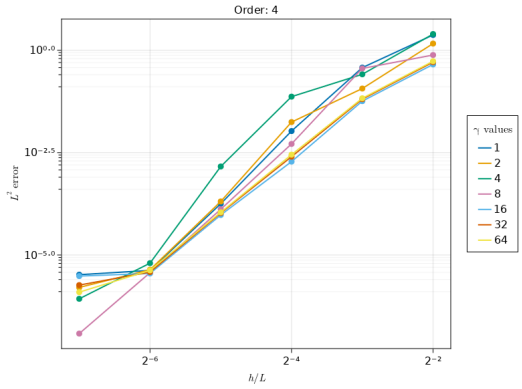

(c)

Figure 4: Convergence study for penalty parameters γ with the model parameters $L = 1$, $m = 7$ and $r = 3$. Figures 4a, 4b and 4c has respectively the order $k = 2, 3, 4$.

As predicted, the EOC matches with the estimates including some numerical artifacts. Lastly, while we cannot provide a theoretical estimate for H^1 norm, the estimate,

$$\|u - u_h\|_{H^1(\Omega)} \lesssim O\left(h^k\right), \quad k \geq 3,$$

seems like a reasonable approximation based on the EOC.

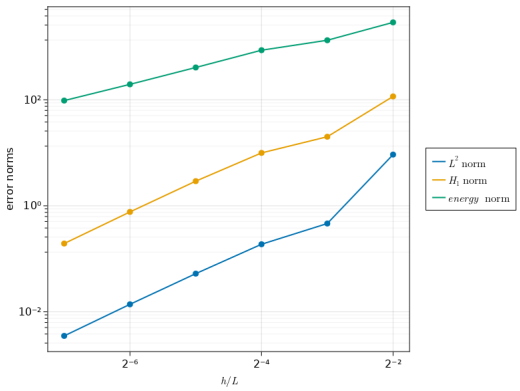

(a)

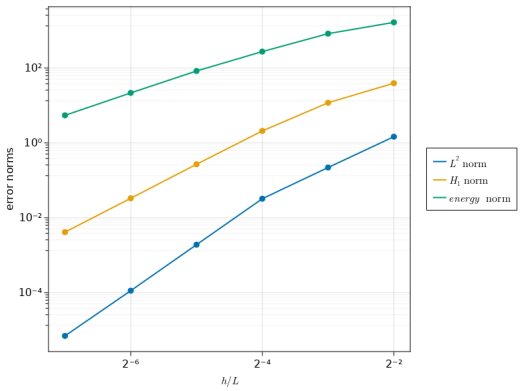

(b)

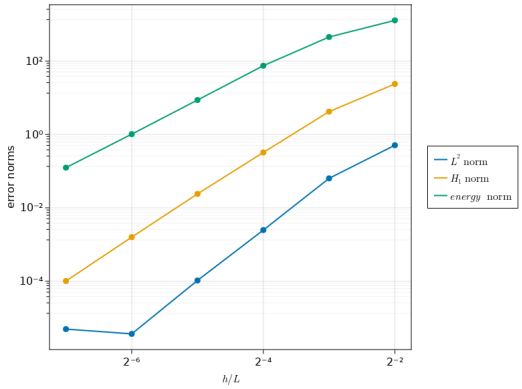

(c)

Figure 5: Convergence plots with model parameters $L = 1$, $m = 7$ and $r = 3$ Figures 5a, 5b and 5c has respectively the order $k = 2, 3, 4$ with penalty parameters $\gamma = 9, 18, 30$.

Table 1: Convergence table with the model parameters $L = 1$, $m = 7$ and $r = 3$ with order $k = 2$ using $\gamma = 9$

i	h/L	L^2 **norm**	**EOC**	H_1 **norm**	**EOC**	**energy norm**	**EOC**
0	$\frac{1}{4}$	9.253E+00		1.158E+02		2.888E+03	
1	$\frac{1}{8}$	4.632E-01	4.320E+00	2.008E+01	2.527E+00	1.328E+03	1.120E+00
2	$\frac{1}{16}$	1.883E-01	1.299E+00	9.954E+00	1.013E+00	8.620E+02	6.238E-01
3	$\frac{1}{32}$	5.250E-02	1.842E+00	2.918E+00	1.770E+00	4.070E+02	1.083E+00
4	$\frac{1}{64}$	1.385E-02	1.922E+00	7.665E-01	1.929E+00	1.957E+02	1.056E+00
5	$\frac{1}{128}$	3.515E-03	1.979E+00	1.941E-01	1.981E+00	9.665E+01	1.018E+00

Table 2: Convergence table with the model parameters $L = 1$, $m = 7$ and $r = 3$ with order $k = 3$ using $\gamma = 18$

i	h/L	L^2 **norm**	**EOC**	H_1 **norm**	**EOC**	**energy norm**	**EOC**
0	$\frac{1}{4}$	1.466E+00		3.942E+01		1.664E+03	
1	$\frac{1}{8}$	2.203E-01	2.735E+00	1.184E+01	1.736E+00	8.318E+02	1.000E+00
2	$\frac{1}{16}$	3.231E-02	2.769E+00	2.092E+00	2.500E+00	2.758E+02	1.593E+00
3	$\frac{1}{32}$	1.910E-03	4.081E+00	2.690E-01	2.959E+00	8.364E+01	1.721E+00
4	$\frac{1}{64}$	1.127E-04	4.083E+00	3.316E-02	3.020E+00	2.171E+01	1.946E+00
5	$\frac{1}{128}$	6.988E-06	4.011E+00	4.131E-03	3.005E+00	5.461E+00	1.991E+00

Table 3: Convergence table with the model parameters $L = 1$, $m = 7$ and $r = 3$ with order $k = 4$ using $\gamma = 30$

i	h/L	L^2 **norm**	**EOC**	H_1 **norm**	**EOC**	**energy norm**	**EOC**
0	$\frac{1}{4}$	5.083E-01		2.377E+01		1.282E+03	
1	$\frac{1}{8}$	6.355E-02	3.000E+00	4.185E+00	2.506E+00	4.516E+02	1.505E+00
2	$\frac{1}{16}$	2.475E-03	4.682E+00	3.223E-01	3.699E+00	7.450E+01	2.600E+00
3	$\frac{1}{32}$	1.050E-04	4.559E+00	2.398E-02	3.749E+00	8.670E+00	3.103E+00
4	$\frac{1}{64}$	3.675E-06	4.837E+00	1.593E-03	3.912E+00	1.018E+00	3.090E+00
5	$\frac{1}{128}$	4.958E-06	-4.319E-01	1.013E-04	3.974E+00	1.246E-01	3.031E+00

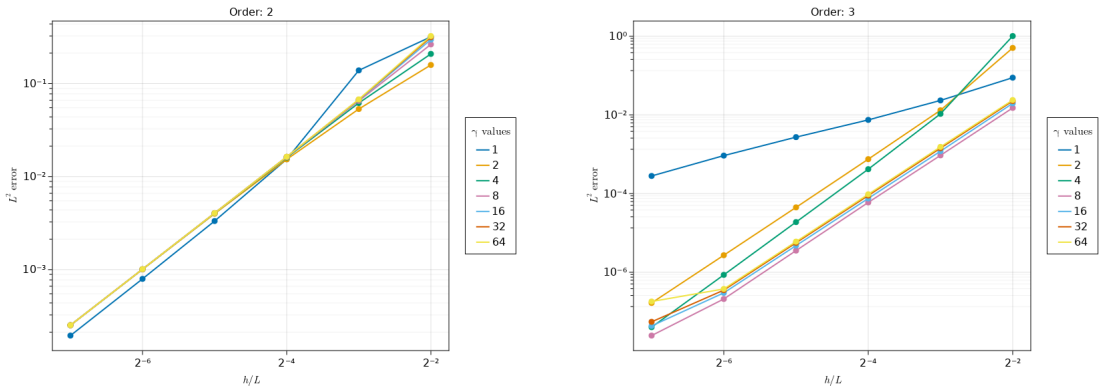

(a) (b)

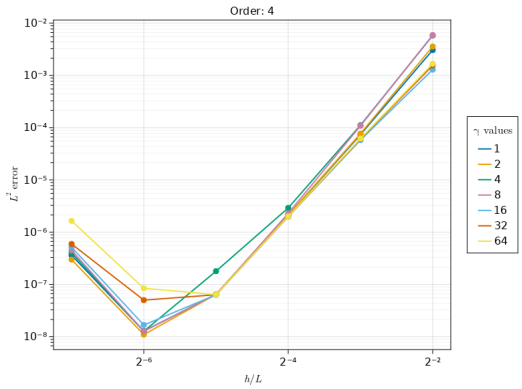

(c)

Figure 6: Convergence study for penalty parameters γ with the model parameters $L = 2\pi$, $m = 1$ and $r = 1$. Figures 4a, 4b and 4c has respectively the order $k = 2, 3, 4$.

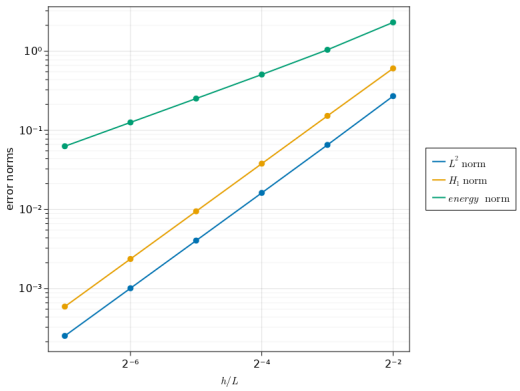

(a)

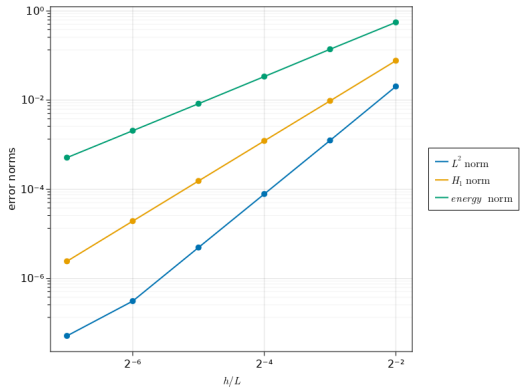

(b)

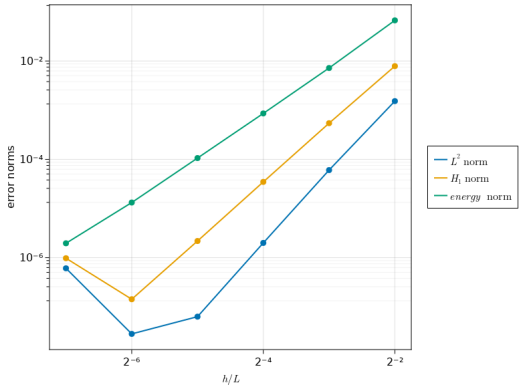

(c)

Figure 7: Convergence plots with model parameters $L = 2\pi$, $m = 1$ and $r = 1$. Figures 7a, 7b and 7c has respectively the order $k = 2, 3, 4$ with penalty parameters $\gamma = 9, 18, 30$.

Table 4: Convergence table with the model parameters $L = 2\pi$, $m = 1$ and $r = 1$ with order $k = 2$ using $\gamma = 9$

i	h/L	L^2 **norm**	**EOC**	H_1 **norm**	**EOC**	**energy norm**	**EOC**
0	$\frac{1}{4}$	2.708E-01		6.068E-01		2.316E+00	
1	$\frac{1}{8}$	6.547E-02	2.048E+00	1.524E-01	1.993E+00	1.043E+00	1.151E+00
2	$\frac{1}{16}$	1.621E-02	2.014E+00	3.796E-02	2.006E+00	5.078E-01	1.039E+00
3	$\frac{1}{32}$	4.041E-03	2.004E+00	9.475E-03	2.002E+00	2.523E-01	1.009E+00
4	$\frac{1}{64}$	1.010E-03	2.001E+00	2.367E-03	2.001E+00	1.260E-01	1.002E+00
5	$\frac{1}{128}$	2.524E-04	2.000E+00	5.918E-04	2.000E+00	6.296E-02	1.001E+00

Table 5: Convergence table with the model parameters $L = 2\pi$, $m = 1$ and $r = 1$ with order $k = 3$ using $\gamma = 18$

i	h/L	L^2 **norm**	**EOC**	H_1 **norm**	**EOC**	**energy norm**	**EOC**
0	$\frac{1}{4}$	2.032E-02		7.678E-02		5.558E-01	
1	$\frac{1}{8}$	1.249E-03	4.024E+00	9.639E-03	2.994E+00	1.387E-01	2.003E+00
2	$\frac{1}{16}$	7.845E-05	3.993E+00	1.219E-03	2.983E+00	3.385E-02	2.035E+00
3	$\frac{1}{32}$	4.946E-06	3.987E+00	1.539E-04	2.986E+00	8.327E-03	2.023E+00
4	$\frac{1}{64}$	3.104E-07	3.994E+00	1.935E-05	2.992E+00	2.063E-03	2.013E+00
5	$\frac{1}{128}$	5.147E-08	2.592E+00	2.427E-06	2.995E+00	5.134E-04	2.007E+00

Table 6: Convergence table with the model parameters $L = 2\pi$, $m = 1$ and $r = 1$ with order $k = 4$ using $\gamma = 30$

i	h/L	L^2 **norm**	**EOC**	H_1 **norm**	**EOC**	**energy norm**	**EOC**
0	$\frac{1}{4}$	1.529E-03		7.869E-03		6.700E-02	
1	$\frac{1}{8}$	6.050E-05	4.660E+00	5.437E-04	3.855E+00	7.205E-03	3.217E+00
2	$\frac{1}{16}$	2.000E-06	4.919E+00	3.482E-05	3.965E+00	8.594E-04	3.068E+00
3	$\frac{1}{32}$	6.335E-08	4.980E+00	2.189E-06	3.992E+00	1.063E-04	3.016E+00
4	$\frac{1}{64}$	2.828E-08	1.164E+00	1.432E-07	3.934E+00	1.325E-05	3.003E+00
5	$\frac{1}{128}$	6.097E-07	-4.430E+00	9.776E-07	-2.772E+00	1.965E-06	2.753E+00

References

[1] A.P.S. Selvadurai. *Partial Differential Equations in Mechanics 2: The Biharmonic Equation, Poisson's Equation*. Springer Berlin Heidelberg, 2013, pp. 1–3,104–105. ISBN: 9783662092057. URL: https://books.google.es/books?id=ct95BgAAQBAJ.

[2] John W. Cahn and John E. Hilliard. "Free Energy of a Nonuniform System. I. Interfacial Free Energy". In: *The Journal of Chemical Physics* 28.2 (1958), pp. 258–267. DOI: 10.1063/1.1744102. eprint: https://doi.org/10.1063/1.1744102. URL: https://doi.org/10.1063/1.1744102.

[3] Junseok Kim et al. "Basic Principles and Practical Applications of the Cahn–Hilliard Equation". In: *Mathematical Problems in Engineering* 2016 (Jan. 2016), pp. 1–11. DOI: 10.1155/2016/9532608.

[4] John B. Greer, Andrea L. Bertozzi, and Guillermo Sapiro. "Fourth order partial differential equations on general geometries". In: *Journal of Computational Physics* 216.1 (2006), pp. 216–246. ISSN: 0021-9991. DOI: https://doi.org/10.1016/j.jcp.2005.11.031. URL: https://www.sciencedirect.com/science/article/pii/S0021999105005498.

[5] Louis W. Ehrlich and Murli M. Gupta. "Some Difference Schemes for the Biharmonic Equation". In: *SIAM Journal on Numerical Analysis* 12.5 (1975), pp. 773–790. DOI: 10.1137/0712058. eprint: https://doi.org/10.1137/0712058. URL: https://doi.org/10.1137/0712058.

[6] Wolfgang Hackbusch. *Elliptic Differential Equations, Second Edition*. 2017, pp. 113–118, 86. URL: https://link.springer.com/content/pdf/10.1007/978-3-662-54961-2.pdf.

[7] Guo Chen, Zhilin Li, and Ping Lin. "A fast finite difference method for biharmonic equations on irregular domains and its application to an incompressible Stokes flow". In: *Advances in Computational Mathematics* 29 (2008). DOI: 10.1063/1.5065188.

[8] Vasily Belyaev and Vasily Shapeev. "Solving the Biharmonic Equation in Irregular Domains by the Least Squares Collocation Method". In: *AIP Conference Proceedings* 2027 (Nov. 2018), p. 030094. DOI: 10.1063/1.5065188.

[9] Zhong-Ci Shi. "Nonconforming finite element methods". In: *Journal of Computational and Applied Mathematics* 149.1 (2002). Scientific and Engineering Computations for the 21st Century - Me thodologies and Applications Proceedings of the 15th Toyota Conference, pp. 221–225. ISSN: 0377-0427. DOI: https://doi.org/10.1016/S0377-0427(02)00531-9. URL: https://www.sciencedirect.com/science/article/pii/S0377042702005319.

[10] S. Brenner and R. Scott. *The Mathematical Theory of Finite Element Methods*. Texts in Applied Mathematics. Springer New York, 2007, pp. 271, 76–77. ISBN: 9780387759340. DOI: 10.1007/978-0-387-75934-0. URL: https://link.springer.com/content/pdf/10.1007/978-0-387-75934-0.pdf.

[11] Devika Shylaja and M. T. Nair. "Conforming and Nonconforming Finite Element Methods for Biharmonic Inverse Source Problem". In: (2021). DOI: 10.48550/ARXIV.2106.07357. URL: https://arxiv.org/abs/2106.07357.

[12] Franco Brezzi and Michel Fortin. "Mixed and Hybrid Finite Element Method". In: *Springer Series In Computational Mathematics; Vol. 15* (Jan. 1991), p. 164. DOI: 10.1007/978-1-4612-3172-1.

[13] F. Brezzi. "On the existence, uniqueness and approximation of saddle-point problems arising from lagrangian multipliers". eng. In: *ESAIM: Mathematical Modelling and Numerical Analysis - Modélisation Mathématique et Analyse Numérique* 8.R2 (1974), pp. 129–151. URL: http://eudml.org/doc/193255.

[14] Susanne Brenner. *C0 Interior Penalty Methods*. Springer International Publishing, 2012. URL: https://link.springer.com/content/pdf/10.1007/978-3-642-23914-4_2.pdf.

[15] Susanne C Brenner et al. "A Quadratic Cˆ0 Interior Penalty Method for Linear Fourth Order Boundary Value Problems with Boundary Conditions of the Cahn–Hilliard Type". In: *SIAM Journal on Numerical Analysis* 50.4 (2012), pp. 2088–2110.

[16] S. Gu. *C0 Interior Penalty Methods for Cahn-Hilliard Equations*. Louisiana State University, 2012. URL: https://books.google.no/books?id=eKP1xQEACAAJ.

[17] A. Manzoni, A. Quarteroni, and S. Salsa. *Optimal Control of Partial Differential Equations: Analysis, Approximation, and Applications*. Applied Mathematical Sciences. Springer International Publishing, 2021. ISBN: 9783030772253. URL: https://books.google.no/books?id=V3NpzgEACAAJ.

[18] A. Quarteroni. "Numerical Models for Differential Problems, Third Edition". In: (). DOI: 10.1007/978-3-319-49316-9. URL: https://doi.org/10.1007/978-3-319-49316-9.

[19] Xiu Ye and Shangyou Zhang. "A conforming DG method for the biharmonic equation on polytopal meshes". In: (2019). DOI: 10.48550/ARXIV.1907.10661. URL: https://arxiv.org/abs/1907.10661.

[20] Robert C. Kirby and Lawrence Mitchell. "Code generation for generally mapped finite elements". In: *CoRR* abs/1808.05513 (2018). arXiv: 1808.05513. URL: http://arxiv.org/abs/1808.05513.

[21] A. Ern and J.L. Guermond. *Theory and Practice of Finite Elements*. Applied Mathematical Sciences. Springer New York, 2004, pp. 69–70. ISBN: 9780387205748. URL: https://books.google.no/books?id=CCjm79FbJbcC.

[22] Francesc Verdugo and Santiago Badia. "The software design of Gridap: A Finite Element package based on the Julia JIT compiler". In: *Computer Physics Communications* 276 (July 2022), p. 108341. DOI: 10.1016/j.cpc.2022.108341. URL: https://doi.org/10.1016/j.cpc.2022.108341.

[23] Jeff Bezanson et al. "Julia: A fresh approach to numerical computing". In: *SIAM Review* 59.1 (2017), pp. 65–98. DOI: 10.1137/141000671. URL: https://epubs.siam.org/doi/10.1137/141000671.

[24] Shuang Li and Kening Wang. "Condition Number Estimates for C0 Interior Penalty Methods". In: (2007). Ed. by Olof B. Widlund and David E. Keyes, pp. 675–682.

[25] G. Engel et al. "Continuous/discontinuous finite element approximations of fourth-order elliptic problems in structural and continuum mechanics with applications to thin beams and plates, and strain gradient elasticity". In: *Computer Methods in Applied Mechanics and Engineering* 191.34 (2002), pp. 3669–3750. ISSN: 0045-7825. DOI: https://doi.org/10.1016/S0045-7825(02)

00286-4. URL: https://www.sciencedirect.com/science/article/pii/S0045782502002864.